Development of an on-line gaschemistry for element 105

Ya Nai-Qi, U. Baltensperger, H. Gäggeler, D. Jost
Paul Scherrer Institut, Villigen, Switzerland

U.W. Scherer, J.V. Kratz, S. Zauner, H.P. Zimmermann
Universität Mainz

M. Schädel, W. Brüchle
GSI Darmstadt

Ch. Lienert, A. Türler
Universität Bern, Switzerland

C.M. Gannett, K.E. Gregorich, H.L. Hall, R.A. Henderson, D.M. Lee, M.J. Nurmia, D.C. Hoffman
Lawrence Berkeley Laboratory, Berkeley

We have developed a continuous separation procedure for short-lived transactinide nuclides based on the formation of volatile bromides. This technique was optimized on the reactor SAPHIR at PSI using short-lived isotopes of Nb and at the 88-inch cyclotron at LBL with isotopes of Ta and Hf. All these elements are considered to be chemical homologues of the transactinide elements 104 and 105.

Fig. 1 shows a schematic of the set-up used. The products were transported with a gas-jet system to a gas-chromatography (GC) tube (quartz) and collected on a quartz wool plug. From there at a temperature of about 900 to 1000 °C volatile bromides (or oxybromides) were volatilized by adding about 100 ml/min $HBr_{(g)}$. In some cases $HBr_{(g)}$ was first bubbled through BBr_3 to increase the bromating strength. The second part of the GC-oven was kept at a variable but isothermal temperature. After the GC-tube the volatile molecules were ejected into a recluster unit and attached onto new aerosols. Through a capillary those separated products were then transported to counting devices. For γ-detection a filter unit was placed on top of a HPGe detector and for α-decaying nuclides the MG-set-up at LBL was used. Here the products were deposited onto thin foils mounted on a 80-position wheel and - from time to time - the collected activity was stepped in front of surface barrier detectors.

Fig. 2 shows the results obtained using nuclides with half-lives of 14 to 32 s. ^{166}Ta and ^{161}Hf were produced in the reactions ^{20}Ne plus $^{nat.}$Eu and ^{144}Sm. The values shown in Fig. 2 are the yields between entrance of the GC set-up and counting device. The main losses occur because of nuclear decay during the relatively time-consuming process of reattachement onto aerosols in the recluster unit. Obviously the chemical yields for Nb and Hf are significantly higher than that for Ta. By adding BBr_3 the yield of Ta could be increased to some extend but still remained lower than expected.

Fig. 3 shows a preliminary result from an application of this technique to a chemical study of element 105, produced in the ^{18}O + ^{249}Bk reaction. The α-spectrum exhibits mainly isotopes of Bi and Po, besides a small contamination due to actinides (e.g. ^{250}Fm). We attribute the α-events between 8.4 and 8.7 MeV to the isotopes ^{262}105 ($T_{1/2}$ = 35 s) and its daughter ^{258}Lr. This assignment is corroborated by the simultaneously measured fission activity.

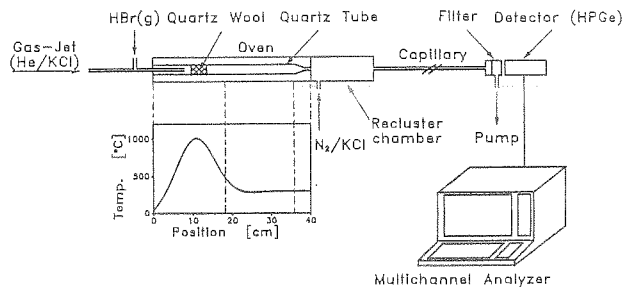

Fig. 1: Gaschromatography set-up used for the separation of volatile bromides

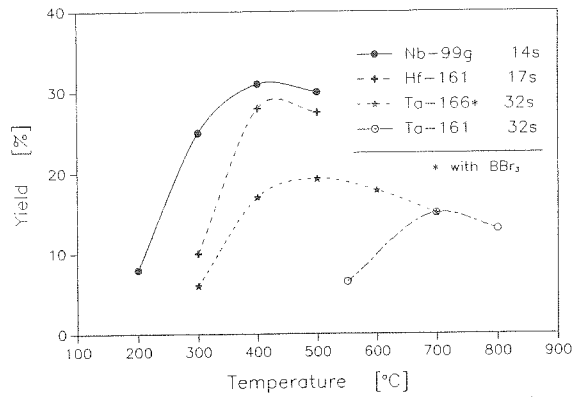

Fig. 2: Chemical yields for volatile bromides of short-lived isotopes of Nb, Ta and Hf.

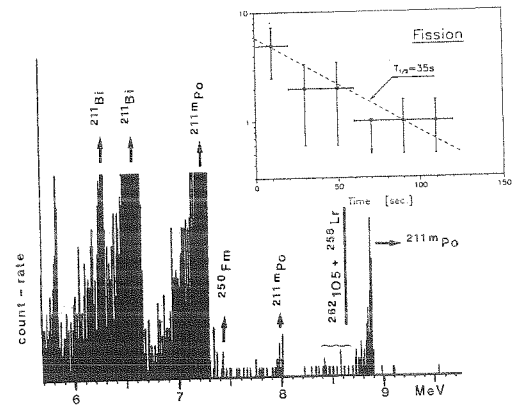

Fig. 3: α-spectrum from a GC-run ^{18}O+ ^{249}Bk measured with the MG-wheel (0-54 s after separation). The GC-temperature was 400 °C and 100 ml/min $HBr_{(g)}/BBr_3$ was used. The inserted part shows the simultaneously measured fission activity.

Alpha- and Spontaneous-Fission Decay of ^{262}Ha [B]

U.W. Scherer, J.V. Kratz, S. Zauner, H.P. Zimmermann
Institut für Kernchemie, Universität Mainz
M. Schädel, W. Brüchle
GSI Darmstadt
C.M. Gannett, K.E.Gregorich, H.L. Hall, R.A. Henderson,
D.M. Lee, M.J. Nurmia, D.C. Hoffman
Lawrence Berkeley Laboratory, Berkeley
U. Baltensperger, H. Gäggeler, D. Jost, Ya Nai-Qi
PSI, Würenlingen
Ch. Lienert, A. Türler
Universität Bern

We produced ^{262}Ha, the longest lived isotope of element 105, in the reaction $^{249}Bk(^{18}O,5n)^{262}Ha$ at the 88-inch cyclotron of Lawrence Berkeley Laboratory. After chemical separation [1] performed with the new microprocessor controlled Automated Rapid Chemistry Apparatus ARCA II [2] the fractions were evaporated on tantalum disks and assayed for α- and SF-activities with Si-surface barrier detectors for 4 min each. We performed about 1600 separations, and observed in a total counting time of about 106 hours some 180 events associated with the decay of 35-s ^{262}Ha and its daughter 4.4-s ^{258}Lr.

The sum spectrum of α-particles observed in those chemical fractions that exhibited ^{262}Ha decays is shown in Fig. 1. Despite the chemical separations that largely eliminated i) huge activities of several Fm and Md isotopes formed in transfer reactions with ^{249}Bk, and ii) Bi and Po activities formed via transfer reactions with a lead impurity in the target, these isotopes are still visible as contaminants in the spectrum. In addition, there is an α-particle group in the energy range 8.3 MeV to 8.7 MeV compatible with the complex spectra [3,4] of ^{262}Ha and its daughter ^{258}Lr. We observed 106 α-decays in this energy window including 15 pairs of correlated decays of ^{262}Ha with subsequent decay of the daughter ^{258}Lr. The half-lives for the different components calculated with maximum likelihood methods are listed in table 1. The single events of ^{258}Lr appear with the half-life of ^{262}Ha being in equilibrium with the mother activity. We may have also observed an unknown α-emitter at 8.49 MeV. The average lifetime of the 15 events assigned to its decay is about 120 s, indicating a random distribution during the counting interval. Therefore, we conclude that the half-life of this component is long compared to the counting time. The nature of this species is unknown, so far.

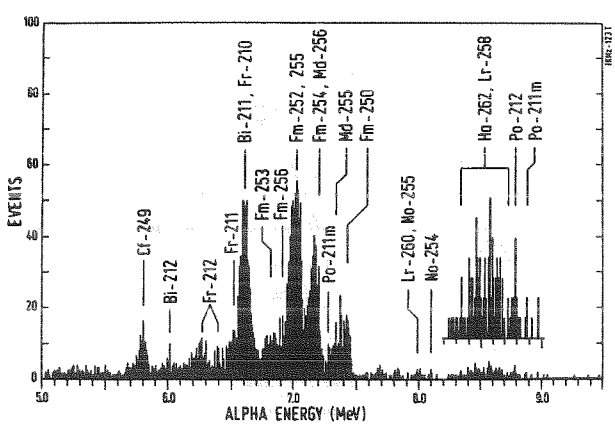

Fig. 1: Sum spectrum of all spectra containing α-events with energies between 8.3 MeV and 8.7 MeV. The insert shows this region intensified.

We also observed 103 fission events. Some of these are due to a small contamination by $^{256}Md/^{256}Fm$. This fraction can be estimated by two independent methods: (i) a decay-curve analysis, and (ii) from the known α/SF ratio of $^{256}Md/^{256}Fm$ and the Fm/Md contamination visible in Fig. 1. Both methods yield in good agreement 12 events for the contribution of $^{256}Md/^{256}Fm$. The half-life of the remaining component, presumably ^{262}Ha, is calculated to be 32.8 ± 6.0 s.

Assuming that α-emission as well as spontaneous fission are decay modes of ^{262}Ha we can calculate the branching ratios. If we consider the unknown 8.49 MeV alpha as coming from ^{262}Ha the fission branch is 46 ± 10 %. With the assumption that this species is a different nuclide the fission branch is calculated to be 50 ± 10 %. Both values are in good agreement with recent results [5].

1. J.V. Kratz et al., contribution to this report
2. M. Schädel et al., contribution to this report
3. A. Ghiorso et al., Phys. Rev. **C4**, 1850 (1971)
4. K. Eskola et al., Phys. Rev. **C4**, 632 (1971)
5. K.E. Gregorich et al., Radiochimica Acta, **43**, 223 (1988)

Species	Half-life (s)	Events
^{262}Ha singles	$39.8 \pm \frac{8.9}{6.2}$	30
^{258}Lr singles	$36.0 \pm \frac{7.9}{5.5}$	31
^{262}Ha corr. mothers	$35.3 \pm \frac{12.3}{7.2}$	15
^{258}Lr corr. daughters	$6.1 \pm \frac{2.1}{1.3}$	15
Fissions	32.8 ± 6.0	91
8.49 MeV α-activity	$83.9 \pm \frac{29.2}{17.2}$	15

Tab. 1: Half-lives of the different components of the α-spectrum in the energy range between 8.3 and 8.7 MeV and the SF component after correction for a small $^{256}Md/^{256}Fm$ component. All the half-lives are compatible with each other and with literature data (See text).

Determination of the Partial Electron Capture- and Spontaneous-Fission Half-Lives of ^{254}No

A. Türler
Universität Bern, Switzerland
H.W. Gäggeler, D.T. Jost
Paul Scherrer Institut, Würenlingen, Switzerland
P. Armbruster, W.Brüchle, H.Folger, F.P.Hessberger, S.Hofmann, G.Münzenberg, V.Ninov, M.Schädel, K.Sümmerer
GSI, Darmstadt
J.V. Kratz, U. Scherer
Universität Mainz

The spontaneous-fission half-lives of even-even transplutonium nuclides exhibit a pronounced maximum at the neutron number N = 152. For elements beyond lawrencium (Z = 103), however, this effect disappears completely[1], see Fig. 1. It is assumed, that this is caused by a change in the structure of the fission barriers, being double humped for Z $\leq$ 102 and single humped for Z $\geq$104. However, for the last nuclide which exhibits this shell effect, ^{254}No, only a lower limit of about 10^5 s for its spontaneous-fission half-life is known. This value was deduced from fusion experiments with light ions where no fission decay from ^{254}No was observed.

We have produced ^{254}No in the reaction ^{208}Pb(^{48}Ca,2n)^{254}No at the UNILAC accelerator at GSI. For separation of fusion products from the primary beam and other reaction products the velocity filter SHIP was used. A rotating target wheel equipped with 0.38 mg/cm^2 metallic ^{208}Pb targets on 40 µg/cm^2 carbon backings was bombarded by typically 5 x 10^{11} p/s of ^{48}Ca. The separated products were implanted into an array of position sensitive surface barrier detectors and assayed for α- and spontaneous-fission decay. The maximum cross section for the production of ^{254}No was found to be (3.25 ± 0.30)µb at a projectile energy of 4.50 MeV/u. During the experiment, a total number of 1615 α-events assigned to the decay of ^{254}No and 11 fission events were accumulated. For these 11 events a half-life of (53^{+46}_{-24})s is deduced at a 95 % confidence level, in good agreement with the literature value for the ^{254}No half-live of 55 s. We did not find any fission from the 0.28 s isomer of ^{254}No, in agreement with theoretical predictions[2]. During the SHIP-bombardment, a long-lived alpha-activity, due to ^{254}Fm, was found. This is indicative of an EC-branch of ^{254}No to ^{254}Md, which then decays by EC to ^{254}Fm. We have therefore performed a chemistry experiment to determine the production cross section of ^{254}Fm, where the products recoiling out of the ^{208}Pb target were collected in a Ni catcher foil. After bombardment this foil was chemically processed. The Cf and Fm fractions were separated from other actinides elements by using HDEHP as stationary phase and were then electroplated on Ta-discs for α- and fission-decay counting. In the Fm fraction the isotopes ^{255}Fm and ^{254}Fm were identified from their α-energy and half-lives. ^{255}Fm is the EC-decay product from ^{255}No, formed in the ^{208}Pb(^{48}Ca,1n)^{255}No reaction.

From the measured α- and spontaneous-fission activities of ^{254}No from the SHIP and the chemistry run we deduce the following branches for the decay channels of ^{254}No: (90 ± 4) % for α, (10 ± 4) % for EC, and $(0.25^{+0.20}_{-0.11})$ % for spontaneous-fission decay. The decay branches as given above lead to the partial half-lives of (61 ± 2) s, (550^{+370}_{-160}) s, and $[(2.2^{+1.8}_{-1.0})]$ x 10^4 s, respectively. Our value for the partial spontaneous-fission half-life is also shown in Fig. 1, indicating that the effect of the N = 152 shell on the spontaneous fission half-life for No is not as pronounced as believed so far.

[1] Yu.Ts.Oganessian et al., JETP., 20, 265 (1974)
[2] A. Baran, Z. Lojewski, Phys. Lett., B176, 7 (1986)

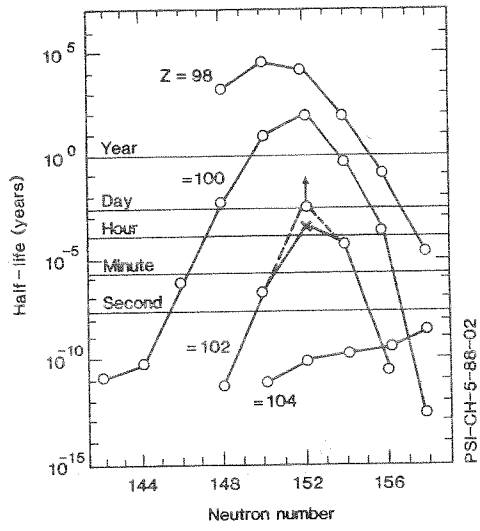

Fig.1: Experimental spontaneous-fission half-lives for even-even nuclides (circle from[1]). The cross shows our result for ^{254}No.

The New Nuclide ^{225}U

F.P.Hessberger, P.Armbruster, W.Brüchle, H.Folger, S.Hofmann, G.Münzenberg, V.Ninov, M.Schädel, K.Sümmerer
GSI Darmstadt

H. Gäggeler, D. Jost
Paul Scherrer Institut, Villigen, Switzerland

J.V. Kratz, U. Scherer
Universität Mainz

M.E. Leino
Universität Helsinki, Finland

A. Türler
Universität Bern, Switzerland

D. Ackermann
TH-Darmstadt

A 270 µg/cm^2 thick metallic ^{180}Hf target was bombarded by a ^{48}Ca beam delivered by the UNILAC accelerator. The beam energy was E/A = 4.24 MeV/u and the average beam intensity about 10 pnA. The evaporation residues were separated in-flight from the primary beam particles and nucleon transfer products by the velocity filter SHIP and stopped in an array of position sensitive surface barrier detectors where the subsequent α-decays were measured. The bombarding energy was close to the Bass-model barrier, which corresponds to an excitation energy $35.5 \leq E^* \leq 37.2$ MeV (given by the target thickness) of the compound nucleus. On the basis of evaporation residue calculations performed with the code HIVAP at this value of E* the 3n-channel should have the highest cross section.

The α-spectrum accumulated in the detector array over a bombarding time of about 6 hours is shown in Fig. 1. Besides a contamination by the long-lived nuclide ^{246}Cf from a previous bombardment two small lines are visible which we attribute to the new nuclide ^{225}U and its granddaughter nuclide ^{213}Rn. This assignment bases on eight α-α correlations found which are summarized in Table 1. Three correlations are complete, i.e. the α-decay attributed to ^{225}U is followed by a pile-up event from ^{221}Th plus ^{217}Ra and an α-decay of ^{213}Rn. We used for the main amplifiers a shaping time constant of 2µs. This resulted in a complete or partial pile-up of the α-decay signals of ^{221}Th with those of its daughter ^{217}Ra ($T_{1/2}$ = 1.6 µs). Since these pile-up events do not have a unique pulse height, they are not sufficient for a conclusive identification. Hence, in this case the observation of the α-decay of ^{213}Rn is necessary. From our data we determine for ^{225}U a half-life of 80^{+40}_{-20} ms (95 % confidence level) and E_α = 7880±20keV (≈ 90 %) and 7830±20 keV (≈ 10 %).

In addition, one correlated event was detected between a decay with E_α = 7.98 MeV and a pile-up event with an energy of 17.3 MeV. This decay chain fits to the isotope ^{222}Th which is the product from the α2n channel. The production cross-section for ^{225}U was determined to be about 100 nb. This value is significantly lower compared to a cross section of about 800 µb found in the reaction $^{176}Yb(^{48}Ca,4n)^{220}Th$[2]. This drastic decrease in evaporation residue cross sections when going from Th to U compound nuclei with similar isospin may be explained by a decrease of the fission barriers of the corresponding nuclei by about 2 MeV as predicted by the CPS model[3].

[1] H.Gäggeler et al., this report, p.
[2] C.-C. Sahm et al., Nucl. Phys. A441, 316 (1985)
[3] S.Cohen et al., Ann.Phys. (NY)82, 557 (1975)

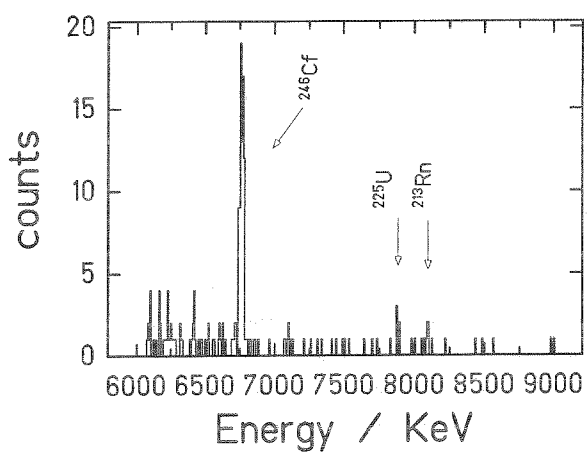

Fig. 1: α-spectrum accumulated during a 6-hour bombardment.

Mother		Daughter 1		Daughter 2	
E_α keV	Δt ms	E_α keV	Δt ms	E_α keV	Δt ms
7873	11			8091	83
7878	22			8091	17
7878	343	8482	4	8088	20
7874	139	16427	5		
7889	50	15681	0.07	8104	8
7873	49	9521	0.19		
7831	62	17232	3	8086	66
7894	239	9006	0.67		

Table 1:
α-α correlations found. Mother = ^{225}U; daughter 1 = ^{221}Th and ^{217}Ra (pile-up); daughter 2 = ^{213}Rn

The Cold Fusion Reaction between ^{48}Ca and ^{208}Pb

H.W.Gäggeler, D.T.Jost
Paul Scherrer Institut, Villigen, Switzerland
A. Türler
Universität Bern, Switzerland
P.Armbruster, W.Brüchle, W.Reisdorf, F.P.Hessberger, S.Hofmann, G.Münzenberg, V.Ninov, M.Schädel, K.Sümmerer
GSI, Darmstadt
J.V.Kratz, U.W.Scherer
Universität Mainz
M.Leino
Universität Helsinki, Finland

Cold fusion reactions with Pb or Bi targets were used in recent years for the synthesis of the heaviest elements up to Z = 109. However, production of those elements is hampered by the increasing hindrance of the fusion process (extra-push) resulting in very low production cross sections, presumably in the sub-picobarn level for $Z \geq 110$. On the other hand, for an accurate prediction of heavy element production rates still many details are unknown such as the influence of structural properties of the reacting nuclei.

We have focused our interest on a study of fusion evaporation residue cross sections using targets ranging from Hf to Bi and ^{48}Ca as projectile. Of special interest is the very cold fusion reaction between the doubly magic nuclei ^{48}Ca and ^{208}Pb. Here, the compound nucleus ^{256}No is produced at the fusion (Bass) barrier with an excitation energy of only 23 MeV. This reaction was already investigated earlier. However, the results from the literature reveal large descrepancies. For separation and detection of Nobelium evaporation residues we have used both the velocity filter SHIP and chemical techniques. The reaction with the highest cross section, ^{208}Pb (^{48}Ca, 2n) ^{254}No, was studied both with the SHIP by detecting the 8.10 MeV α-line of ^{254}No but also chemically by determining the cross section for ^{246}Cf, a long-lived grand-daughter of ^{254}No. The neighbouring channel ^{208}Pb (^{48}Ca, 1n)^{255}No was measured by chemistry, assuming the nuclide ^{255}No to decay by 35,5 % to the long-lived grand-daughter ^{255}Fm. A direct detection of ^{255}No by SHIP is somewhat hampered by the fact that its main α-line is - within resolution - identical to the α-line of ^{254}No, which is produced with a much higher cross section.

The nuclide ^{253}No from the 3n-channel was determined with SHIP by its 8.01 MeV α-line.

All results are shown in Fig. 1. We observe a very narrow excitation function for the 2n-channel with a FWHM of only about 5 MeV and a maximum cross section of 3.25 ± 0.30 μb. This FWHM-value is significantly lower compared to the neighbouring reactions ^{208}Pb (^{40}Ar, 2n) ^{246}Fm or ^{208}Pb (^{50}Ti, 2n) $^{256}104$, which have a FWHM of about 10 MeV[1,2]. On the other hand the maximum cross section of 3.25 μb is by two to three orders of magnitude higher compared to the corresponding values of the reactions mentioned above.

An analysis of the data shown in Fig. 1 with HIVAP indicates that this system doesn't yet show any hindrance of the fusion process ("extra-push") despite the rather high fissility x(Blocki) = 0.792 but also seems to have a zero variance σ_B^2 of the fusion barrier B.

[1] F.P.Hessberger et al., GSI-87-1, p.17 (1987)

[2] F.P.Hessberger et al., Z.Physik A321, 317 (1985)

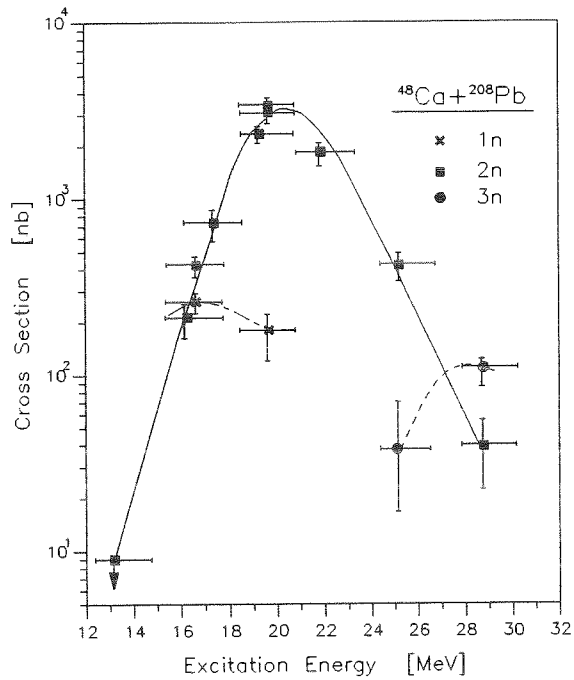

Fig.1: Excitation functions for evaporation residues produced in the fusion process between ^{48}Ca and ^{208}Pb

Cross Section Calculations of Hot Fusion Evaporation Residues with HIVAP

M. Schädel

GSI Darmstadt

It seems to be clear that the hindrance of the fusion process at the barrier is presently the limiting effect for the so far successful synthesis of the heaviest elements in cold fusion reactions[1]. To understand this hindrance effect more quantitatively, see Ref. 2, and to base cross section estimates for the **hot fusion** as a possibly alternative path on solid grounds, a systematic comparison of a large number of experimental data with calculated cross sections has been performed.

The goal of this investigation was to find out to which extent the results from the code HIVAP are in agreement with experimental data (i) if evaporation residues in various xn-channels for the same target-projectile combination are populated (excitation energy dependence), (ii) if many isotopes of the same element are produced in combination of targets and projectiles with different masses but fixed atomic number (isotope dependence), and (iii) if increasingly heavy elements are formed with targets and projectiles varying as little as possible from one compound nucleus to the next (element dependence).

HIVAP was used with **one** set of standard parameters. This set has never been changed for all the calculations, which is of crucial importance if systematic trends should be devulged. In this brief contribution not all the parameters can be discussed but the most sensitive ones should be mentioned. Firstly, no additional shell correction or an additional factor for the liquid drop barrier has been introduced (SHELL = 0, BARFAC = 1), and secondly, for the shell damping energy the default value (EDAMP = 18) has been used.

Excitation functions for 4n through 8n evaporation channels from the $^{238}U(^{12}C,xn)^{250-x}Cf$ reaction are shown in Fig.1. Very good agreement between the experiment[3] and the calculation is achieved not only for the position of the maxima but also for the absolute cross section values.

A comparison of experimental data from $^{244;246;248}Cm(^{12;13}C,\mathbf{4n})^{252\text{-}257}No$ reactions[4] with calculations has revealed that there is no significant isotope dependent variation visible. The ratio between calculated and measured cross sections is shown in Fig.2. The maximum deviation, which is observed for ^{257}No, is a factor of 0.4.

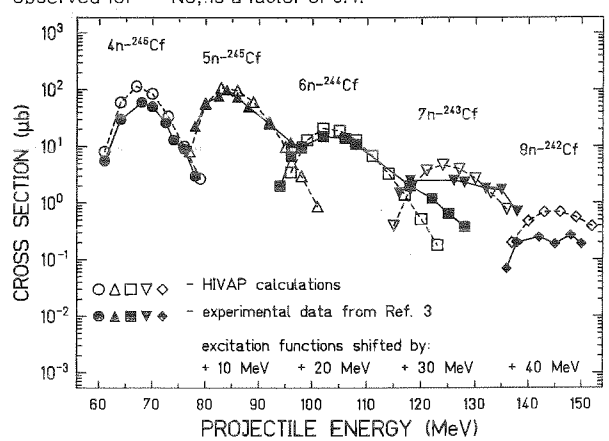

Fig.1: Excitation functions for the $^{238}U(^{12}C,xn)^{250-x}Cf$ reaction.

Obviously HIVAP provides an excellent description of isotope production for Cf and No isotopes. Its potential for the prediction of heavy element production in hot fusion reactions has been tested up to the $^{249}Cf(^{18}O,4n)^{263}106$ reaction; $^{263}106$ being the heaviest nuclide synthesized in a hot fusion reaction. From an inspection of Fig. 3 it is clear that up to the heaviest element HIVAP gives, within a factor of 2, a good agreement between calculation and experiment. It also shows that there is no significant fusion hindrance observable for the $^{263}106$ production, as a fusion hindrance would reduce the experimental cross section. Finally, it is interesting to note that almost all of the investigated experimental excitation functions exhibit a high energy tail which can with no means be reproduced in the calculations.

1. P. Armbruster, Ann. Rev. Nucl. Part. Sci. 35, 135 (1985)
2. W. Reisdorf, contribution to this report
3. T. Sikkeland et al., Phys. Rev. C169, 1000 (1968)
4. T. Sikkeland et al., Phys. Rev. 172, 1232 (1968)
5. K. Eskola et al., Phys. Rev. C4, 632 (1971)
6. J.M. Nitschke et al., Nucl. Phys. A352, 138 (1981)
7. A. Ghiorso et al., Phys. Rev. Lett. 24, 1498 (1970)
8. V.A. Druin et al., Sov. J. Nucl. Phys. 25, 591 (1979)

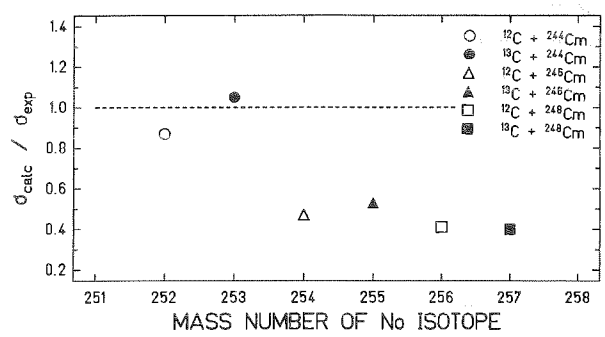

Fig.2: Ratio between calculated and experimental cross sections for various No isotopes.

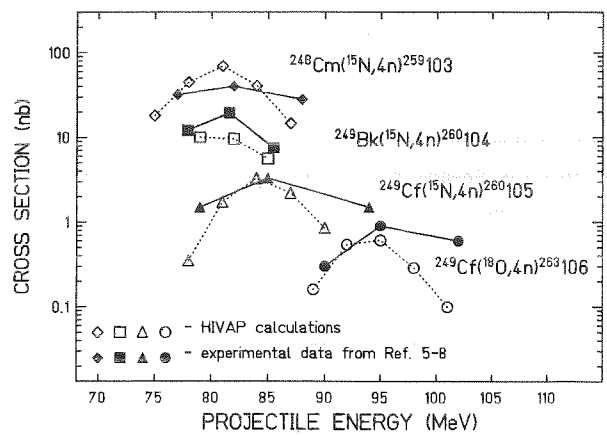

Fig.3: Comparison of calculated and measured excitation functions for heavy element production in hot fusion reactions.

Competition of Direct Reactions with Fusion [B]

R. Bellwied, J.V. Kratz
Institut für Kernchemie der Universität Mainz
W. Reisdorf, D. Schüll
GSI Darmstadt
B. Kohlmeyer
Universität Marburg
R. Künkel
HMI Berlin

We have previously reported /1/ on radiochemical determinations of mass- and charge distributions in collisions of ^{86}Kr with ^{76}Ge ($Z_1Z_2 = 1152$), ^{104}Ru ($Z_1Z_2 = 1584$), and ^{130}Te ($Z_1Z_2 = 1872$), i.e. in collision systems that span the region from unhindered fusion to a massive dynamical hindrance of fusion (extra-push) at near-barrier energies. Direct reactions in the unhindered system Kr+Ge constitute of just two narrow (quasi-elastic) transfer peaks. At the extra-push threshold (Kr+Ru) the valley between these transfer peaks is beginning to be filled by reactions with large mass flow toward symmetry, and above threshold (Kr+Te) this fission-like process covers a range of 70 mass units and has increased to a cross section of about 30 mb. More dramatic, on an absolute scale, is the concurrent increase of the cross sections in the narrow transfer peaks from 40 mb (Ge) through 100 mb (Ru) to 280 mb (Te). Together with other sub-barrier or near-barrier transfer cross sections converted /1/ (where necessary) to the same incident energy (E/B = 1.0) and to the average Q_{gg}-value (-3.5 MeV) these cross sections are shown as open circles in Fig. 1 as a function of Z_1Z_2. The rise of the transfer cross sections above $Z_1Z_2 = 1600$ coincides with the onset of fusion hindrance at this point.

Our new measurements at the GSI magnetic spectrometer of direct reaction cross sections in the collisions of 4.15 MeV/u ^{96}Zr and ^{124}Sn ions with ^{90}Zr and ^{96}Zr, respectively, corroborate the steep rise of the quasi-elastic transfer cross sections in the vicinity of $Z_1Z_2 = 1600$. In the previous radiochemical measurements, no dynamical information on the degree of energy damping associated with the direct reaction channels was available, and the distinction of "quasi-elastic" transfers from more complex transfers had to be performed on the basis of their mass distributions. The new data include total kinetic energy loss (TKEL)-spectra for all reaction channels /2/, and it was decided to separate quasi-elastic from more inelastic transfers at TKEL < 12 MeV. This energy loss corresponds to the difference between the entrance channel energy and the average exit channel fusion barrier. The integral quasi-elastic transfer cross sections defined this way are indicated as crosses in Fig. 1. The resulting complete cross section balance for the two new systems is shown in Tab.1. The new data underline the important role of quasi-elastic reflections from the diabatically rising barrier /3/ for trajectories that would normally lead to complete fusion. However, it is important to emphasize that, in addition, there are more complex, and more dissipative binary collisions, and finally, fission-like processes that also compete with complete fusion /2/.

1. R. Bellwied et al., GSI 87-1, p.46 (1987)
2. R. Bellwied et al., this report, also thesis Univ. Mainz
3. D. Berdichevsky, A. Lukasiak, W. Nörenberg, P. Rozmej, Preprint GSI-88-70 (1988)
4. C.C.Sahm et al., Nucl. Phys. A441, 316 (1985)

cross section balance / [mb]		
channel	$^{124}Sn \rightarrow {}^{96}Zr$	$^{96}Zr \rightarrow {}^{90}Zr$
$\sigma(1n)$	54.3±5.0	40.2±6.2
$\sigma(2n)$	17.6±1.9	15.4±1.9
$\sigma(3n)$	6.2±1.2	4.3±3.0
$\sigma(1p)$	14.0±2.1	11.2±1.9
$\sigma(2p)$	3.3±0.8	5.7±1.3
$\sigma(1p,1n)$	10.68±1.4	8.1±2.0
$\sigma(1p,2n)$	10.35±1.8	6.0±1.4
$\sigma(1p,3n)$	4.8±0.8	-
$\sigma(2p,3n)$	7.0±1.1	-
$\sigma(2p,4n)$	5.2±0.9	-
$\sigma(\alpha)$	8.8±0.9	-
$\sigma(3p,3n)$	2.7±0.5	-
$\sigma(quasi-elastic)$	205±20	122±20
$\sigma(deep-inelastic)$	60±20	≤ 20
$\sigma(fission-like)$	40±10	≤ 10
$\sigma(evap.residues)$	≤ 2	15±5
$\sigma(inelast.excit.)$	67±10	84±20
$\sigma(reaction)$	430±100	300±80
$\sigma(q.e.(converted))$	205±20	95±20

Tab.1: Cross section balance for the two new systems.
The first part shows cross sections for selected dominant transfer channels. These cross sections correspond to pickup-channels for ^{124}Sn + ^{96}Zr and to stripping channels for ^{96}Zr + ^{90}Zr.
The second part shows the actual cross section balance. The separation into a quasi-elastic, a deep-inelastic and a fission-like part is described in /2/. These data are complemented by evaporation residue cross sections from the SHIP-group /4/, and measurements of the inelastic excitation.
For comparison we evaluate a value for the reaction cross section (σ(reaction)) by an optical model fit.
The last column shows the converted quasi-elastic transfer cross sections, which are used in the systematics, see Fig.1.

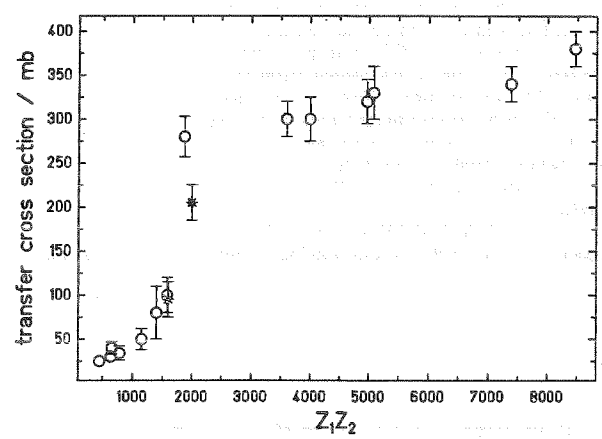

Fig.1: Quasi-elastic transfer cross sections in heavy ion collisions as a function of Z_1Z_2 for an incident energy of E/B = 1.0. The crosses indicate new measurements in the systems ^{96}Zr + ^{90}Zr and ^{124}Sn + ^{96}Zr. The open circles correspond to various sub- and near-barrier transfer measurements /1/.

Transition from Quasi-Elastic to Completely Relaxed Reactions in a System with Dynamically Hindered Fusion: $^{124}Sn + ^{96}Zr$ [B]

R. Bellwied, J.V. Kratz
Institut für Kernchemie der Universität Mainz
W. Reisdorf, D. Schüll
GSI Darmstadt
B. Kohlmeyer
Universität Marburg
R. Künkel
HMI Berlin

We have previously reported /1/ on integral mass and charge distributions in collisions of ^{96}Zr with ^{90}Zr and ^{124}Sn with ^{96}Zr near the respective fusion barrier: For the heavier system nucleon exchange towards more complex transfer channels is increased. This is correlated with an increasing hindrance of fusion /2/. In order to further assess the dynamical properties of these reseparation channels we have focused on the energy-loss spectra (TKEL = -Q) in the reaction 4.15 MeV/u $^{124}Sn + ^{96}Zr$ which was performed at the GSI magnetic spectrometer. These data should provide important information on the nature of the dynamical hindrance to fusion at near-barrier energies.

The measurements were carried out in inverse kinematics in the angular range $5° \leq \Theta_{lab} \leq 40°$ in 5° steps. The target-like reaction products show increasing inelasticity with decreasing laboratory angle. The grazing angle corresponds to $\Theta_{lab} = 30°$. Fig. 1 shows TKEL distributions at $\Theta_{lab} = 25°$ for various nuclear charges around the target. Indicated by the arrows are i) the values of TKEL for full energy damping (Viola energy), and ii) the expected location of the exit channel fusion barrier. From the distributions it is obvious that there is a dynamical transition from quasi-elastic to more inelastic transfer reactions with increasing nucleon exchange. Fig. 2 shows a comparison of the measured mass distribution at $\Theta_{lab} = 20°$ without any TKEL-restriction, and for TKEL > 40 MeV. The latter distribution is broadened, and its maximum is shifted to smaller masses, i.e. to larger mass asymmetry.

There is also a smooth transition of this deep-inelastic distribution into a fission-like distribution of mass-symmetric fragments. For a restricted range of Z-values ($42.5 \leq Z \leq 47,5$), the fission component is well separated from the transfer distribution, see Fig.1. Based on the cross section observed in this window and on an estimate of its width in the frame of fission systematics, one obtains a flat fission cross section over the whole angular range. The separation between quasi-elastic and deep-inelastic collisions is done on the basis of the exit channel barrier, which corresponds to TKEL < 12 MeV for Z = 40. Fig.3 shows the angular distributions for the three different reaction channels: The reaction is dominated (205 mb) by quasi-elastic transfers of a few nucleons with an angular distribution peaked around the grazing angle. Then, with a tendency for orbiting, there is the deep-inelastic component. Unfortunately, the experiment was not able to include the whole angular range for this channel. With the differential cross section restricted to the measured angular range and complemented by an upper limit for $\Theta_{CM} = 140\text{-}180°$ one obtains a total cross section of 60 mb. Third, there is the fission-like component with a total cross section of about 40 mb. This is to be compared with a fusion cross section of ≤2 mb, if estimated from the data of ref./2/, and of about 200 mb for unhindered fusion (Bass barrier). Adding to the 100 mb of deep-inelastic plus quasi-fission cross section, the 'surplus' quasi-elastic cross section (~100 mb) suggested by the transfer systematics discussed in a separate report /3/, we can tentatively account for the missing flux in the fusion cross section.

It might well be that there is a competition of three dynamical processes - in order of decreasing importance - i) quasi-elastic reflection from the diabatically rising barrier /4/, ii)dissipation in the approach phase /5/ lowering the kinetic energy below the fusion barrier energy and involving complex transfers, and iii) passage over the barrier and friction in the chaotic regime dynamics /6/.

1. R. Bellwied et al., GSI report 88-1, p.38 (1988)
2. C.C. Sahm et al., Nucl. Phys. A441, 316 (1985).
3. R. Bellwied et al., this report, and thesis Univ. Mainz
4. D. Berdichevsky, A. Lukasiak, W. Nörenberg, P. Rozmej, Preprint GSI-88-70 (1988).
5. P. Fröbrich, Phys. Reports 116, 337 (1984).
6. J.W. Swiatecki, Nucl. Phys. A376, 471 (1982).

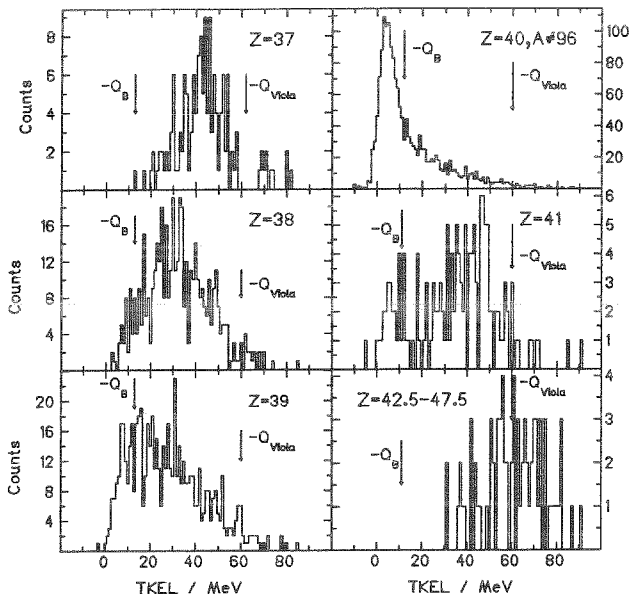

Fig.1: Energy loss distributions at $\Theta_{lab} = 25°$ for various nuclear charges around Z = 40. The arrows indicate the location of the fusion barrier in the exit channel ($-Q_B$) and total energy damping based on Viola-systematics ($-Q_{Viola}$).

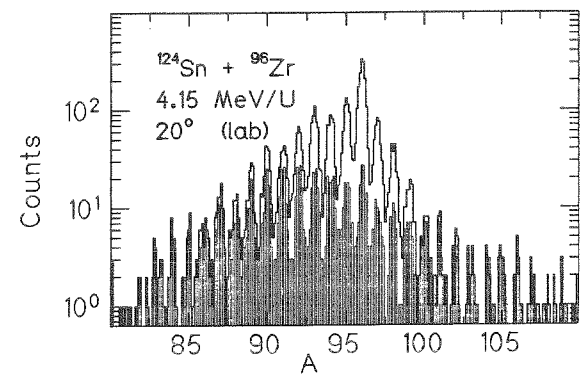

Fig.2: Comparison of mass distributions for $\Theta_{lab} = 20°$ without any TKEL restriction (open histogramm) and for TKEL > 40 MeV (full histogramm).

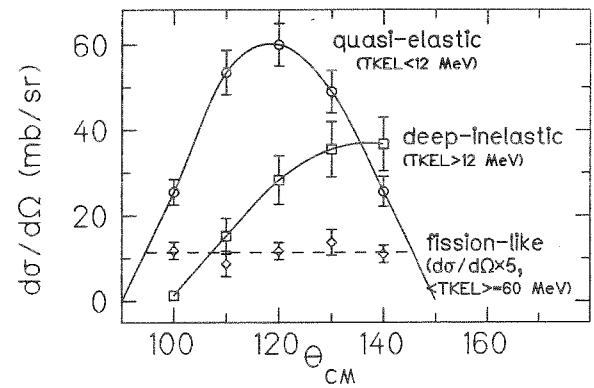

Fig.3: Angular cross section distributions for various reaction channels with smooth curves to guide the eye.

Nuclear Reactions in U + U and U + Au Collisions below and near the Coulomb Barrier

G. Wirth, W. Brüchle, Fan Wo, E. Jäger and K. Sümmerer
GSI Darmstadt
F. Funke, J.V. Kratz, and N. Trautmann
Institut für Kernchemie, Universität Mainz

Experiments investigating nuclear reactions in very heavy ion collisions at energies below and near the classical Coulomb barrier V_C were continued with special emphasis on the question of nuclear contact and the search for prolonged interaction times. The collision dynamics between very heavy ions at low energies is dominated by the strong repulsive Coulomb interaction. Effects from the static deformation of the collision partners, the dynamic deformations of the colliding nuclei and the strong localisation of single reaction channels in the relative distance could influence the potential resulting in a pocket. It is therefore not clear under which kinematic conditions nuclear contact is reached and whether collisions with prolonged interaction times do occur.

One-neutron transfer is the most probable channel with mass transfer in the reaction of very heavy ions at low energies. The angular distributions can be described by the tunneling of a neutron over large distances within a semiclassical theory assuming classical trajectories[1] and should be sensitive to deviations from Rutherford trajectories. A search for the formation of long-lived giant nuclear molecules in the collision U + Au at selected energies near the Coulomb barrier gave negative results[2]. But in order to see resonance scattering the beam energy must fit very precisely the unknown position of such a possible small pocket in the potential and therefore a search at all energies within reasonable limits must be performed. As an advantage, our experiment can use targets of 360 $\mu g/cm^2$ thickness thus integrating in each irradiation the energy bin from the energy loss of the beam in the target of $E_{LAB}/A = 0.08$ MeV/u without increasing the background. Experimentally we have scanned the beam energy in the interval 5.6 MeV/u $\leq E_{LAB}/A \leq$ 6.3 MeV/u in steps of 0.05 MeV/u which yields a sufficient energy overlap between the various irradiations. Additionally two irradiations were performed at 5.4 and 6.56 MeV/u. No indication was found for deviations of the angular distributions for the one-neutron transfer product from the semiclassical theory assuming Rutherford trajectories and therefore there is no evidence for prolonged interaction times. This result does not exclude generally the existence of delayed interaction times in U + Au collisions at low energies because the one-neutron transfer channel must not necessarily couple to these collisions. It might be possible that during long contact times the probability for the transfer of several nucleons is much higher compared to the transfer of a single neutron.

In a previously published measurement of the fission excitation function[3] we have attributed the high fission cross sections exceeding the expected cross sections for Coulomb fission in U + U collisions to sequential fission following multi-nucleon transfer. It was concluded that multi-nucleon transfer takes place already at low energies, $(0.90 \pm 0.02) \times V_C$. The finite fission widths associated with the decay of such multi-nucleon transfer products requires, for consistency, the positive identification of surviving products from the transfer of many nucleons. In order to search for these survivors and in order to gain additional insight into the reaction mechanism we have measured excitation functions for the formation of several radiochemically accessible Ra, Ac and Th isotopes. Examples are shown in Fig.1. The products were stopped in catcher foils, separated chemically, and prepared as weightless samples for α-particle spectroscopy. The excitation functions for (2p,xn), (3p,xn), and (4p,xn) transfers are very similar to each other and suggest that the observed isotopes are members of a broad product distribution which is similar in both reactions U + U and U + Au. It has to be checked whether the characteristics of these distributions are compatible with what is known for damped collisions thereby indicating the onset of neck formation already at these low beam energies.

1. G. Wirth et al., Phys. Lett. **B177**(1986)282
2. G. Wirth et al., GSI Scientific Report 1987, **88-1** (1988)42
3. G. Wirth et al., Z. Phys. **A330**(1988)87

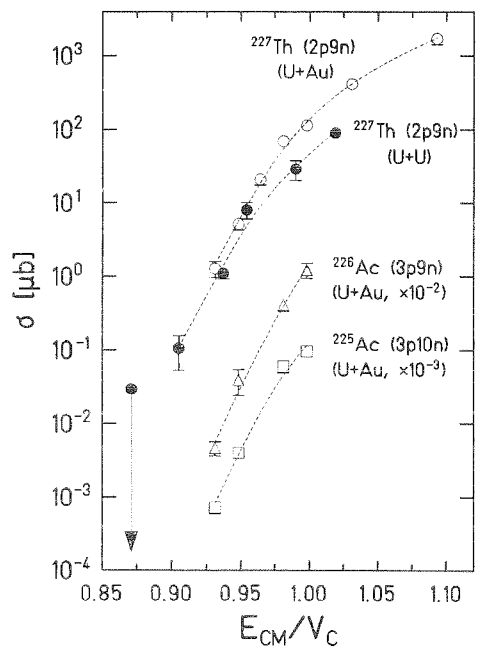

Fig. 1: Excitation functions for complex transfer reactions in the systems U + U and U + Au. The lines are drawn to guide the eye.

Radiochemical Cross Section Measurements of Spallation Products from Au and Th Targets

K. Sümmerer, W. Brüchle, D.J. Morrissey, M. Schädel, B. Szweryn and Yang Weifan
GSI Darmstadt

Radiochemically determined spallation cross sections measured for collisions of relativistic protons and heavy ions with many different targets are up to now the basis of estimates of projectile fragmentation cross sections at SIS energies. A parametrization of such data with an empirical function[1] has proven to be a useful tool for such estimates, at least for light and medium mass projectiles. The scarcity of experimental cross sections, however, made extrapolations of such estimates into the region of heavier nuclei very uncertain. We have therefore performed a radiochemical study of proton-induced spallation of Au and Th targets to obtain more and better experimental data for heavy nuclei, with the emphasis on **independent** cross sections, i.e. those that are not modified by β-decay.

Several irradiations of Au and Th targets have been performed with the 2.6 GeV proton beam of the SATURNE accelarator at Saclay/France. After the irradiations, the targets were immediately chemically processed and the resulting chemical fractions assayed with γ-ray spectroscopy. Details of these procedures have been published recently[2].

In addition to a large number of cumulative cross sections that were partly already known from a similar experiment[3] at 3 GeV we have obtained many new independent cross sections. As in all activation experiments, these data are somewhat scattered since only few isotopes have suitable decay characteristics. Nevertheless, we conclude that for spallation products sufficiently removed from the Au target (e.g. the Lu and Tm isotopes shown in Fig.1) the empirical function of Ref.1 seems to reproduce the experimental cross sections reasonably well.

To understand better the physics of high-energy proton-nucleus collisions, we have performed calculations with the internuclear-cascade-plus-evaporation code ISABELLE of Yariv and Fraenkel[4]. If fission is completely switched off in the evaporation part of the calculation, the isotope distributions are similar in shape and height as the empirical function of Ref.1, but shifted slightly towards the neutron-rich side (the same observation has been made for medium-mass nuclei). On the other hand, for fragments close to the Au target the empirical formula of Ref.1 is not a good approximation. Here, the ISABELLE calculation seems to be the better approach.

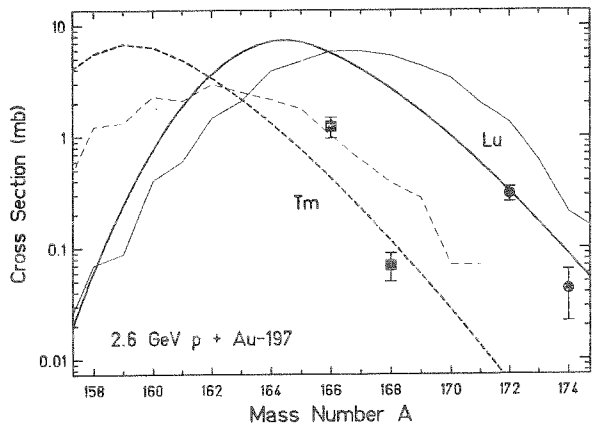

Fig.1:
Measured independent isotope distributions for lutetium (circles) and thulium (squares) from reactions of 2.6 GeV protons with gold. The thick curves indicate the prediction of the empirical function of Ref. 1 for Lu (full lines) and Tm (dashed lines), respectively. The thin lines represent calculations with the ISABELLE code of Ref. 4.

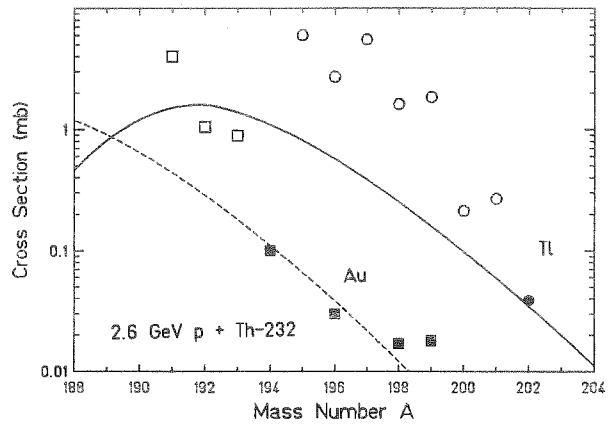

Fig.2:
Measured independent (full symbols) and cumulative (open symbols) isotope distributions for thallium (circles) and gold (squares) from reactions of 2.6 GeV protons with thorium. The curves represent the prediction of Ref.1 multiplied by a factor of 0.27.

The irradiation of a Th target and the subsequent analysis of Tl and Au fractions were meant to provide an estimate how fission depletes the prefragment distribution formed in the fast (internuclear cascade) step of the proton-nucleus collision in the case of very fissile nuclei. As has been noted previously (e.g. Ref. 5 and references therein), a surprisingly large fraction of the prefragments decay by particle evaporation instead of fission at very high excitation energies. This is reflected in the observation that the Tl and Au isotope distributions from Ref. 1 (which neglect any fission competition) reproduce nicely the measured independent cross sections if multiplied by a factor of 0.27 (Fig.2). This means that only 2/3 of the excited prefragments in p+Th reactions are lost due to fission and about 1/3 survive. This observation indicates that there is a good chance to produce new neutron-rich heavy nuclei by Th and U projectile fragmentation at SIS/FRS.

1. K. Sümmerer et al., GSI Scientific Report 1986, GSI-87-1 (1987), p.97
2. B. Szweryn et al., Radiochimica Acta, in press (1988)
3. S.B. Kaufman et al., Phys. Rev. *C 22* (1980) 167
4. Y.Yariv et al., Phys. Rev. *C 20* (1979) 2227
5. H. Delagrange et al., Z. Physik *A 323* (1986) 437

Search for strange matter by Rutherford backscattering [B]

K.Lützenkirchen, S.Polikanov, C.Sastri
GSI Darmstadt
G.Herrmann, M.Overbeck, N.Trautmann
Institut für Kernchemie, Universität Mainz
A.Breskin, R.Chechik, Z.Fraenkel, U.Smilansky
Weizmann Institute, Rehovot, Israel

According to a number of suggestions stable strange matter could exist in the form of supermassive nuclei (or "strange nuggets")[1,2]. A piece of strange matter is expected to be a mixture of "up", "down", and "strange" quarks in about equal proportions. Small amounts of strange matter could have survived from the early stages of the Universe[1] or might reach the Earth as a flux of strange nuggets produced in collisions of neutron stars [3]. Here we report some results of a search for supermassive nuclei by using Rutherford backscattering of heavy ions[4].

In our experiments natural samples were irradiated with beams of ^{238}U and ^{208}Pb nuclei at an energy of 1.4 MeV/u. This energy is far below the Coulomb barrier of nuclei so that the cross section for nuclear reactions is negligible, and the interaction of nuclei is dominated by elastic scattering. In this case the angle and the velocity of the scattered projectile nucleus are determined by the mass of the target nucleus. In a single scattering event a projectile can be scattered into the backward hemisphere only by a heavier nucleus. Therefore, ^{238}U or ^{208}Pb observed at angles 90^{o}-180^{o}would indicate the presence of more massive and possibly strange nuclei.

In the present study scattered nuclei were detected in a system of twelve low-pressure multi-wire proportional counters[5] divided into four identical modules each of which consisted of one start and two stop detectors. The ranges of scattering angles covered by this system are 92^{o}-120^{o} and 127^{o}-170^{o} with a total solid angle of 1.15 sr. Detected nuclei are identified by measuring the time-of-flight (TOF) and the specific ionization (ΔE). The scattering angle is obtained from the position measurements in start- and stop-detectors.

A thick target ($\simeq$1 g/cm^2) prepared from an iron meteorite (Sam's Valley meteorite, Medford, Oregon, 1894) was irradiated with $1.7*10^{14}$ particles of ^{238}U. Figures 1a and b show the two-dimensional spectra of ΔE versus TOF of particles in the angular regions 92^{o}-120^{o} and 127^{o}-170^{o}, respectively. No data were recorded below ΔE$\simeq$110 (in relative units) due to an electronic cut-off.

The solid curves in Fig.1a,b represent the 2σ-range (95.4% probability) of ΔE-TOF values for ^{238}U scattered from a thin uranium target in a calibration experiment. From Figs. 1a,b we can see that no scattered uranium nuclei were recorded with TOF below 90 ns. While some uranium nuclei with TOF above 90 ns are seen at 92^{o}-120^{o} (Fig.1a), no uranium nuclei were recorded at angles exceeding 127^{o} (Fig.1b). This strong decrease in the number of scattered nuclei with angle is typical for multiple scattering, and for this reason the events with TOF above 90 ns were excluded from the further analysis. The absence of events between TOF$\simeq$30 ns, which corresponds to the initial velocity of uranium nuclei, and 90 ns can be used to estimate limits for the abundance of supermassive nuclei in a certain mass range. Its lower end is determined by TOF = 90 ns, which corresponds to backscattering of uranium from nuclei with mass A$\simeq$400 located at the target surface.

A group of scattered nuclei centered around 70-80 ns with specific ionization much lower than that for uranium ions of the same velocity was observed at angles 92^{o}-120^{o} (Fig.1a). This group was identified as nuclei with Z$\simeq$30. and assigned to iron nuclei. They can result from rescattering of iron recoil nuclei produced in primary uranium-iron collisions.

The resulting limits for the abundance of supermassive nuclei with masses $A \cong 4*10^{2}$-10^{7} amu relative to the number of nucleons are ranging from 10^{-10} to 10^{-14}. The main trend of increasing sensitivity with increasing mass results from the increasing Rutherford cross section (the charge Z, which determines σ_{Ruth}, increases with A, see Ref.2). We did not extend the estimated limits beyond $A \geq 10^{7}$ since more reliable information on the screening of the nuclear charge by electrons inside a large strange nugget would be required.

Our limits for the abundance of strange matter are close to some instructive estimates by De Rujula and Glashow[3] which are mainly based on the assumption that all local dark matter consists of strange nuggets. At the present stage we do not consider it useful to put constraints on these theoretical considerations. The reason is that for the sample investigated here we cannot exclude appreciable fluctuations in the concentration of supermassive nuclei caused by fractionations during chemical processes in the early Universe.

1. Witten, E. Phys. Rev. **D30**, 272-285 (1984).
2. Farhi, E. & Jaffe, R.L. Phys. Rev. **D30**, 2379-2390 (1984).
3. De Rújula, A. & Glashow, S.L. Nature **312**, 734-737 (1984).
4. Brügger, M. et al. Nature(London), in press.
5. Breskin, A. et al. GSI Scientific Report 1987, p.343.
6. Northcliffe, L.C. & Schilling, R.F. Nucl.Data Tables **A7**, 233 (1970).

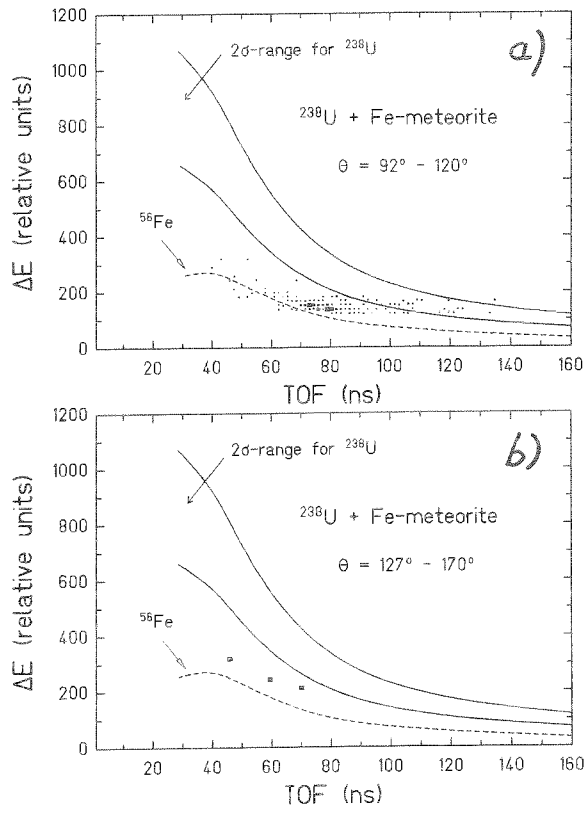

Fig.1 ΔE versus TOF. The points represent 245 (a) and 3 (b) detected particles. Dashed line : Calculated[6] locus of ^{56}Fe nuclei. Solid lines : 2σ-range for scattered ^{238}U from a calibration experiment.

Elution of Lanthanides and Actinides with α-Hydroxy-Isobutyrate from Cation Exchange Columns Revisited

M. K. Gober, J. V. Kratz, U. W. Scherer
Institut für Kernchemie der Universität Mainz

For ions of the same charge and hydration number in a given chromatographic system the logarithm of the distribution coefficient, $logK_D$, is a linear function of the ionic radius [1]. We made use of this linear correlation in the recent determination of the ionic radii and hydration enthalpies of Md^{3+} and Lr^{3+} ions [2], for which the elution positions from a cation exchange(CIX) column using ammonium-α-hydroxyisobutyrate(α-HIB)-solutions (pH =4.85) at 80°C were measured relative to the elution positions of the lanthanide ions Tm^{3+}, Er^{3+}, and Ho^{3+}.

The linear correlation of $logK_D$ *vs.* ionic radius is expected to break down when the hydration (coordination) number CN is changed. From the measurement of diffusion coefficients for several Ln^{3+} and An^{3+} ions at 25°C it is known [3] that a change of CN from 8 to 9 occurs around Eu^{3+} in the lanthanide series and around Bk^{3+} in the actinide series with the smaller value of CN being associated with the heavier elements in both series. For higher temperatures measurements of CN are not available, and it was argued [4] that the discontinuity might then occur at lower atomic number . This should cause a temperature-dependent discontinuity in the correlation of $logK_D$ *vs.* ionic radius also in α-HIB/CIX separations. The published K_D-values for 87°C [5] and for 25°C [6] are not necessarily compatible with this proposition. Therefore, we have considered it worthwhile to remeasure systematically the elution positions of Ln^{3+} and An^{3+} ions from CIX columns with α-HIB solutions at both room temperature and 87°C.

Lanthanide tracer activities and actinides were either produced by reactor irradiations, obtained commercially, or were produced by heavy-ion bombardements. Mixtures of the tracers were dissolved in ~100μl of a 0.025M α-HIB solution and were added to our standard HPLC system through a sample loop and absorbed on top of a 2×60mm column packed with Aminex A6 cation exchange resin (particle size 17.5 ± 2μm) kept at 25°C or 87°C, respectively. They were subsequently eluted from the column with α-HIB solution. Concentration and pH of the α-HIB solutions were varied, because elution of all Ln^{3+} and An^{3+} ions with the same α-HIB would lead to poor separation of the heavy elements and unreasonably long times for eluting the lighter elements, which would elute in very broad peaks. So the lanthanides and actinides were divided in groups of up to eight elements, each group being eluted at an optimum concentration and pH of the α-HIB. The effluent assayed for γ- and α-activity in order to determine the distribution of the lanthanide and actinide tracer activities. From the retention volumes associated with the peak maxima of the elution curves the logarithm of the distribution coefficients, $logK_D$, were determined as a function of the ionic radius [7] of the Ln^{3+} and An^{3+} ions. The combined results of repetitive experiments at 25°C, and at 87°C, respectively, are shown in figs. 1 and 2. Renormalizations of the elution positions of the Ln^{3+} and An^{3+} ions to a common pL-value (negative logarithm of the ligand concentration determined from the α-HIB concentration and its dissociation equilibrium at the given pH) were performed by using the logarithmic dependence of K_D on pL. At 87°C such renormalizations were performed for La^{3+} only. At 25°C it was necessary to renormalize the values for Pm^{3+} through La^{3+}. A comparison of Figs. 1 and 2 shows the break in the linear correlations of $logK_D$ *vs.* ionic radius occurs at the same position at both temperatures with the transition between the two linear sections being broadened at the higher temperature. This broadening does not extend into the Tm^{3+}, Er^{3+}, and Ho^{3+} region where the ionic radii of Md^{3+} and Lr^{3+} had been determined previously [2].

1. Y. Marcus, A.S. Kertes, Ion Exchange and Solvent Extraction of Metal Complexes, Wiley,1969, p. 287
2. W. Brüchle et al., Inorg. Chim. Acta 146, 267 (1988)
3. F. David, J. of the Less Common Metals **121**, 27 (1986)
4. F. David, private communication
5. G. H. Higgins, The Radiochemistry of the Transcurium Elements, U.S. NAS-NS-3031,1960
6. H.L. Smith, D.C. Hoffman, J. Inorg. Nucl. Chem.,3, 243 (1956)
7. D. H. Templeton, C. H. Dauben, JACS 76, 5237 (1954)

Figure 1:

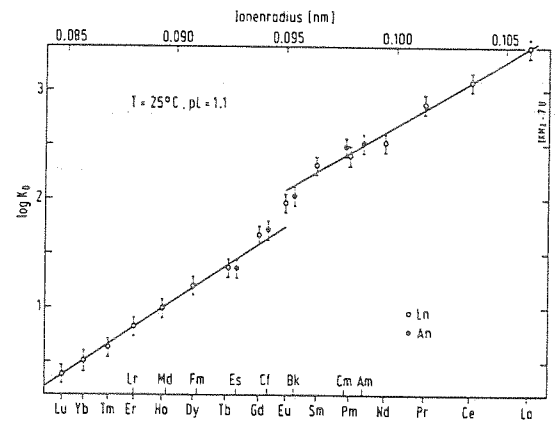

Figure 2:

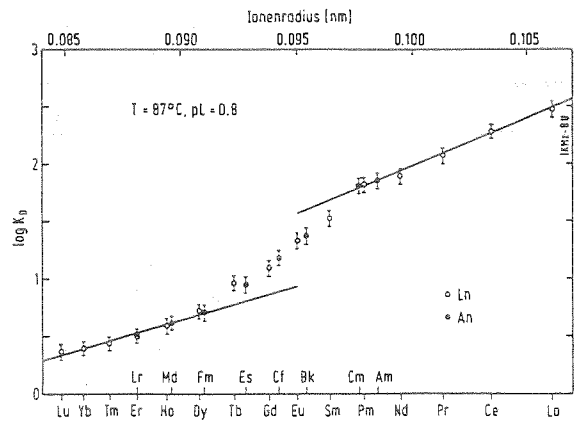

Thermochromatography of Carrier-free Iridium and Platinum[B]

F. Zude, W. Fan, N. Trautmann, G. Herrmann

Institut für Kernchemie, Universität Mainz

In view of a rapid and continuous chemical separation procedure for the superheavy elements with Z = 109 and 110 the volatility of carrier-free amounts of their homologues iridium and platinum in a dry and moist stream of oxygen has been studied.

The thermochromatographic apparatus has been described in a previous paper[1]. Typical conditions for the experiments were: flow-rate of 10 - 30 l/h O_2, linear negative temperature gradient of 18° C/cm and starting temperatures between 900 and 1000° C. Either a dry gasstream with less than $5 \cdot 10^{-5}$ Pa H_2O or with a humidity of 79 Pa was used. The distribution of the iridium and platinum activity along the thermochromatographic column was determined by γ singles measurements.

Carrier-free amounts of Ir-188 ($t_{1/2}$= 41.5 h) and Ir-189 ($t_{1/2}$=13.1 d) and of Pt-191 ($t_{1/2}$= 2.8 d) were produced by (α,xn)-reactions from rhenium foils or osmium powder, respectively, at the KfK Karlsruhe cyclotron.
For the separation of iridium the rhenium target was dissolved in hot concentrated nitric acid and the rhenium was completely removed by extraction into tetraphenylarsonium chloride dissolved in $CHCl_3$. Carrier-free platinum was obtained after dissolving the osmium target in aqua regia and evaporating osmium in form of the very volatile OsO_4, followed by an extraction of $H_2[PtCl_4]$ into ether.

A thermochromatogram of iridium and platinum with a dry oxygen stream of 20 l/h and an exposure time of 15 min is shown in figure 1. In order to obtain reproducible results it was necessary to volatilize first the iridium sample by an oxidation step with 15.4 l/h dry O_2 in a thermochromatographic column with a temperature gradient of -150° C/cm. Here the activity was collected in a small zone of 4 cm on the quartz surface. Then this iridium sample was either directly evaporated in dry or moist oxygen or after a reduction in a gas stream of 5.3 l/h H_2 at an oven temperature of 650° C. The adsorption temperatures and adsorption enthalphies ΔH_a for iridium are listed in table 1. The adsorption enthalphy ΔH_a has been estimated from the adsorption temperature according to Eichler [2] with an adsorption entropy ΔS_a of -180 $Jmol^{-1}K^{-1}$. In dry oxygen the adsorption enthalphy is compatible with the literature value of 129 ± 4 $kJmol^{-1}$. In moist oxygen two adsorption peaks as described by Domanov and Eichler [3] were obtained only after the reduction step. In the literature [3] a value of 105 ± 4 $kJmol^{-1}$ is given for the adsorption enthalpy of the lower temperature peak which is in agreement with our data.

Platinum in carrier amounts could not be volatilized under the descibed conditions. With carrier-free platinum a volatile compound was obtained with an adsorption temperature of 445 ± 25° C as seen in figure 1. The corresponding adsorption enthalphy is - 177.8 ± 6.2 $kJmol^{-1}$, while in the literature [3] a value of - 133 ± 4 $kJmol^{-1}$ is reported.

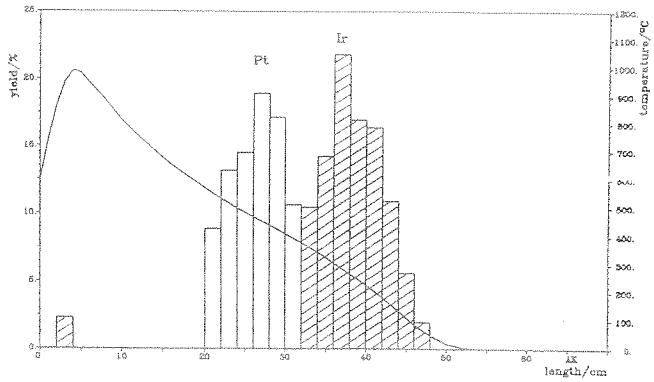

Figure 1: Thermochromatogram of iridium and platinum in a dry oxygen stream of 20 l/h, reduction and an exposure time of 15 min

gas stream	T_A /°C	ΔH_a/ $kJmol^{-1}$
dry oxygen	252 ± 34	- 134.6 ± 8.7
moist oxygen	320 ± 106	- 152 ± 27
dry oxygen	240 ± 25 [a]	- 129.7 ± 6.3
moist oxygen	I 303 (38%) [b]	- 145.7 ± 6.3
	II 160 (46%)	- 109.5 ± 6.3
dry oxygen	I 306 (30%) [b]	- 146.4 ± 6.3
	II 150 (56%)	- 107 ± 6.3

Table 1: Adsorption temperatures und adsorption enthalpies of iridium in an oxygen stream of 20 l/h and after an exposure time of 15 min

a) with a reduction step in dry H_2

b) with a reduction step in moist H_2

References:

[1] F. Zude, N. Trautmann, G. Herrmann, Jahresbericht 1988, p. 4

[2] B. Eichler, I. Zvara, Sov. Radiochem. 30, 233 (1982)

[3] V.P. Domanov, B. Eichler, I. Zvara, Radiochim. Acta 26, 66 (1984)

Spontaneous Deposition of Polonium on Silver

M. Schädel, B. Schausten, W. Brüchle

GSI Darmstadt

W. Weber

IBM Sindelfingen

The determination of alpha-radioactive isotopes in environmental samples has already been of importance for a long time. More recently after the first report about so called soft errors [1], attention is also payed to the possible impact of α-active impurities to metal oxide semiconductors (MOS) and especially to random access memories (RAM).

It was reported that the charge used to determine bit state could be upset and altered by alpha radiation coming from trace elements in a ceramic package, with the result that a bit is switched from a 1 to a 0, or vice versa. The appearance of soft errors may become increasingly important with the development of memories with higher densities, and here not only the packing material or silicon wafers, but also all the chemicals used in the production process may introduce critical amounts of alpha active impurities, mainly the isotopes of elements thorium and uranium with all their daughter activities in the decay chains.

We have started to evaluate the potential of the spontaneous deposition (plating) procedure [2] of Po on Ag-foils as a separation and preparation method to obtain samples for an α-assay. For this procedure, high yields are reported if the solution is boiled with a reducing agent like SO_2 or hydrazine, and variations in the plating efficiency are reported for various acids like HNO_3, H_2SO_4 and acetic acid. We have studied the dependence of Po deposition on Ag as a function of the volume and the time of deposition.

In our standard procedure, we have diluted 333 ml conc. HCl which contained the ^{210}Po-tracer with 500 ml H_2O, added 157 g NaOH, checked with methylred that the solution is still acidic, added 67 g sodium acetate, 50 g $NH_2OH{\cdot}HCl$, and 167 ml H_2O. The pH of the solution at that time was between 4.5 and 5. Aliquot parts of this solution were given into a destillation flask and a (15 × 15) mm² Ag-foil (26 mg/cm²) was inserted. The solution was kept at boiling temperature under reflux conditions for the time of the experiment. At the end, the solution which then had a pH of about 3 was discarded, the Ag-foil was washed with water and acetone, dryed, and the alpha activity was measured on both sides of the foil with a 2π-proportional counter.

In Fig. 1 we show the dependence of the deposition yield as a function of the volume for volumes between 10 ml and 500 ml. A fixed plating time of 3 hours was chosen.

The time dependence of the deposition yield for a solution with a total volume of 300 ml is shown in Fig. 2. All data points are average values from 5 or 6 experiments at each individual time and volume and the error bars represent a ± 1σ value.

It is evident, from an inspection of Fig. 1 and 2, that high deposition yields of 90% and higher can be obtained either by long plating times of about 24 hours, if larger volumes have to be handled or by small volumes of 20 ml or less, with the advantage of much shorter times needed. If one wants to obtain the highest possible sensitivity, for example, when monitoring reagents for chemical processes, the best values with the least expense can be reached from larger volumes and longer times rather than doing many short runs. In a routine analysis, assuming after the deposition an additional 24 h counting period in a 2π proportional counter and the observation of a net counting effect of 20 alphas above a background of 100 alphas, this would result in a detection limit of $1{,}2 \times 10^{-2}$ pCi of ^{210}Po in 300 ml HCl which corresponds to $2{,}7 \times 10^{-18}$ g or $2{,}7 \times 10^{3}$ atoms.

1. T.C. May, M.H. Woods, 16th Ann. Proc., Reliability Physics 1978 (Symp.San Diego) 16, p.33.
2. P.E. Figgins. The Radiochemistry of Polonium, NAS-NS 3037, 1961, p.29.

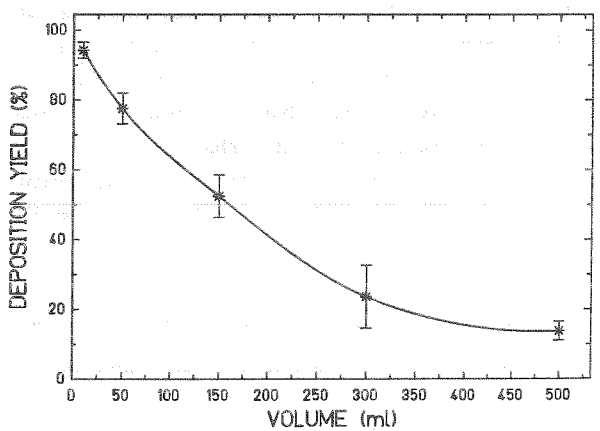

Fig.1:

Yield of ^{210}Po deposition on Ag within three hours as a function of volume. The curve is drawn to guide the eye.

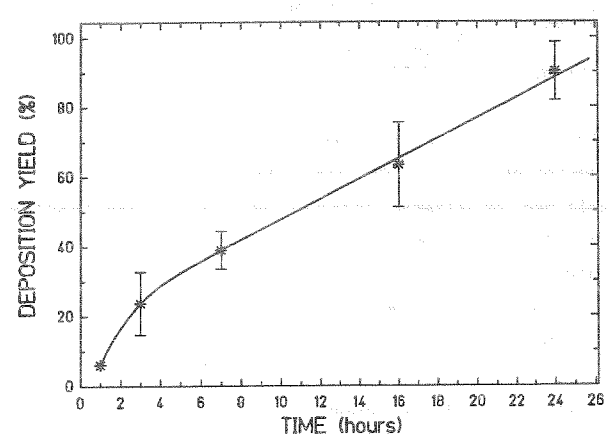

Fig.2:

Yield of ^{210}Po deposition on Ag from 300 ml solution as a function of time. The curve is drawn to guide the eye.

Aqueous Chemistry of Element 105: Adsorption on Glass

K.E. Gregorich, R.A. Henderson, D.M. Lee, M.J. Nurmia, R.M. Chasteler,
H.L. Hall, D.A. Bennett, C.M. Gannett, R.B. Chadwick,
J.D. Leyba, D.C. Hoffman
Lawrence Berkeley Laboratory, Berkeley
G. Herrmann*
Institut für Kernchemie, Universität Mainz, and GSI Darmstadt

The expected ground state electronic configuration of element 105, hahnium, is $[Rn]5f^{14}6d^{3}7s^{2}$. The ionization of hahnium in aqueous solution is expected to stop with the $[Rn]5f^{14}$ core intact, leading to a Ha^{5+} oxidation state that probably exists as a hydrolyzed or complex species such as MO_2^{+}. The aqueous phase chemistry of hahnium would therefore be analogous to that for the group V elements niobium and tantalum. Trends in chemical properties should thus continue to hahnium as the heaviest group V element. However, relativistic effects may cause significant deviations due to a stabilization of low spin electronic orbitals. Stabilization of 7s electrons may lead to Ha^{3+} with a $[Rn]5f^{14}7s^{2}$ configuration.

Due to lack of any pertinent information for hahnium we decided to attempt a first investigation of its aqueous chemistry. The choice of experimental techniques is limited by the short half-lives and low production rates of hahnium isotopes. As a characteristic chemical property we used the strong adsorption of group V elements on glass surfaces from strong nitric acid solutions which is a consequence of the strong tendency of these elements to hydrolyse even in strong acids. Efficient adsorption of carrier-free niobium has been observed in rapid filtration through glass fiber filters of its solutions in strong nitric acid[1]. This behaviour has been used in separations of short-lived niobium nuclides from fission products[2,3].

We verified the strong adsorption with niobium and tantalum isotopes produced by charged-particle induced reactions in on-line experiments carried out under very similar conditions as for the experiments with hahnium. Under the same conditions the group IV elements zirconium and hafnium showed much weaker adsorption. On platinum surfaces the adsorption was generally found to be lower for all these four elements, and on teflon surfaces only tantalum was sticking in a significant fraction.

For the experiments with hahnium, 34-s ^{262}Ha was produced at the LBL 88-inch Cyclotron by the ^{249}Bk(^{18}O,5n) reaction. The reaction products which recoiled out of the target were stopped in helium gas seeded with potassium chloride aerosols. The activity was swept through a capillary to the collection site and collected on a thin glass plate. Then, the glass plate was removed from the collection site and placed on a hot plate. The potassium chloride spot on the glass plate was fumed with 3 µl of 15 M nitric acid. After drying a second fuming was performed with 7 µl of nitric acid. Then, the potassium nitrate and the actinide activities were removed from the glass plate by washing with dilute nitric acid and finally with acetone. After drying, the glass plate was placed on one of a series of Si(Au) surface barrier detectors. The average time from the end of the accumulation of the aerosol to the beginning of counting for alpha and spontaneous fission decays was 51 s.

801 adsorption experiments were performed in the ^{18}O + ^{249}Bk bombardments. The decontamination from actinide elements was very good. Only 0.25% of the fermium activities remained on the glass. During the first 140 s, a total of 26 alpha events was observed in the energy range 8.42 to 8.70 MeV where the complex spectra of the 34-s ^{262}Ha with its daughter 4.3-s ^{262}Lr are located. A spectrum is presented in Figure 1. These 26 events contain 5 time-correlated parent-daughter pairs, as well as about 14 uncorrelated events and about two background events. A maximum likelihood fit of the time distribution gives a half-life of 28^{+7}_{-5} s, consistent with the reported ^{262}Ha half-life of 34±4 s. We also observed 26 spontaneous fission decays in the first 140 s, of which about 3 are background. A half-life of 32^{+8}_{-6} s and a branching ratio of 49±13% is found for the spontaneous fission decay branch. In the chemical experiments the spontaneous fission activity was observed to be about three times smaller than in on-line measurements without any chemical separation. This discrepancy may be due to the production of another activity with a similar half-life that does not accompany hahnium in the adsorption process.

To summarize: Comparison of the ^{262}Ha alpha decay rate from the chemical experiments with that from measurements of unseparated samples indicates a very high sorption yield for hahnium under conditions which lead also to strong adsorption of the group V elements niobium (42% yield) and tantalum (80%) but not for the group IV elements zirconium (0%) and hafnium (11%).

* Visiting Miller Research Professor, University of California, Berkeley, spring 1987

[1] M. Weis, H. Ahrens, H.O. Denschlag, M. Fariwar, G. Herrmann, N. Trautmann, Radiochim. Acta 42 (1987) 201
[2] H. Ahrens, N. Kaffrell, N. Trautmann, G. Herrmann, Phys. Rev. C14 (1976) 211
[3] M. Weis, H.O. Denschlag, J. Inorg. Nucl. Chem. 43 (1981) 437

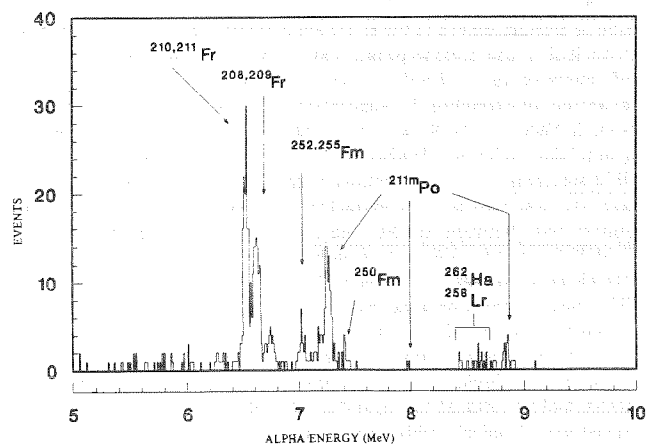

Fig. 1. Summed spectrum of all alpha data from the first 30 s counting from the 801 adsorption experiments of ^{262}Ha-^{262}Lr on glass from concentrated nitric acid solutions.

Extraction of Zr, Nb, Hf, Ta and Pa into Aliphatic Amines [B]

H.P. Zimmermann, P. Klein, J.V. Kratz, U.W. Scherer, S. Zauner
Institut für Kernchemie, Universität Mainz

The chemical behaviour of element 105, hahnium, was studied for the first time only recently [1]. 35-sec $^{262}_{105}$Ha produced by the $^{249}_{97}$Bk ($^{18}_{8}$O, 5n) reaction was used to study the adsorption of hahnium on glass surfaces and to use this as a rapid separation procedure characteristic of a group-5 element. In a second approach, the extraction of hahnium from fluoride solutions into an organic solvent was attempted [1]. The extraction of niobium and tantalum from acidic fluoride solutions into methyl isobutyl ketone (MIBK) is well known. Surprisingly, the fluoride complexes of element 105 could not be extracted into MIBK under conditions in which tantalum (probably present as $[TaF_6]^-$) was extracted quantitatively [1]. Perhaps, the most obvious explanation is the formation of poly-negative anions such as $[HaF_7]^{2-}$. The higher charge would then prevent extraction even into solvents with a relatively high dielectric constant like MIBK.

It is possible to test this proposition by new experiments, in which anionic complexes of element 105 are extracted into high molecular weight amines. This extraction by anion exchange is not restricted to monovalent anions. In order to prepare such experiments, we have performed a systematic study of the extraction behaviour of the group-4 elements Zr and Hf, and of the group-5 and pseudo group-5 elements Nb, Ta and Pa from mineralic acid solutions into various aliphatic amines such as Amberlite XLA-3, tri-n-octyl amine (TOA), tri-iso-octyl amine (TIOA), tri-caprylyl amine (Alamine 336), and methyl-tri-caprylyl ammonium chloride (Aliquat 336). VOLTALEF powder (grain size 125 - 250 μm) was coated with the amine (2:1) which was transformed into the respective ammonium salt by shaking with H_2SO_4, HNO_3, HCl and HF respectively. The tracers ^{95}Zr, ^{95}Nb, ^{181}Hf, ^{182}Ta and ^{233}Pa were stored in 1m HF solution. These were added to 2 ml of mineralic acid solution containing excess hydroboric acid (if the extraction was to be performed in the absence of fluoride ions), and the aqueous phase was contacted with 0.5 g of the VOLTALEF/ammonium salt powder by shaking for 15 min. An aliquot of the aqueous phase was then used to determine the degree of extraction of the tracers into the organic phase by γ-ray counting.

Among the various mineral acid-amine combinations the systems TIOA/HCl or TIOA/HCl/HF were found to be most advantageous for the purpose envisaged. Fig.1, as an example, shows the distribution of the group-5 and group-4 elements between HCl/0.03 M HF and TIOA as a function of the HCl molarity : There is no appreciable extraction of Zr and Hf into the amine even from strong HCl solutions. Ta is extracted quantitatively above 0.2 M HCl. Also, both Nb and Pa begin to be extracted at this point, however, the trend is reversed above 0.4 M HCl due to a displacement of the metal-ion complexes by ion-pair formation with HCl in the organic phase. Later, above 4 M HCl, the formation of doubly charged $[MeOCl_5]^{2-}$ complexes sets in which leads to their quantitative extraction for concentrations > 10 M HCl. Thus, the system is highly suited for a common extraction of the group-5 elements (hopefully including element 105) into the amine from concentrated HCl solutions, while the group-4 elements (including element 104) and the actinides are not extracted. The system also allows one to differentiate between Ta, Nb, and Pa at lower HCl molarities, e.g. at 4 M HCl, and thus offers the possibility to determine the proximity of the chemical properties of element 105 to either of its lighter homologs. The most efficient back-extraktion of Ta into the aqueous phase was found to occur in 6 M HNO_3 / 0.015 M HF.

Next, these extraction data were used to perform High Performance Liquid Chromatography (HPLC) separations of these elements and to optimize the separation with respect to separation factors, speed and chemical yields. Fig.2 shows the elution curves for Zr, for Nb and Pa and for Ta in a manually performed separation. The column size was 1.7 x 11mm and the stationary phase consisted of finely grained VOLTALEF powder coated with TIOA, weight ratio 5:1. The final speeding up of the separation was achieved by automatic separations using the newly designed miniaturized Automatic Rapid Chemistry Apparatus ARCA II [2] .

[1] K.E. Gregorich et al., Radiochim. Acta, 43,223(1988)
[2] M. Schädel et al., contribution to this report

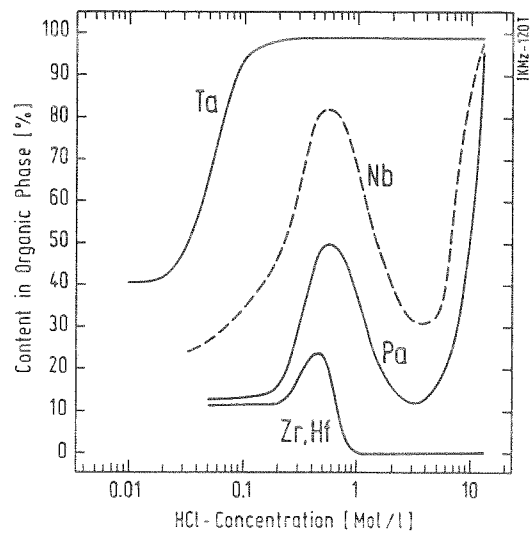

Figure 1: Extraction behaviour of Zr, Nb, Hf, Ta and Pa in the TIOA/HCl system in the presence of 0.03 M HF as determined in batch extractions.

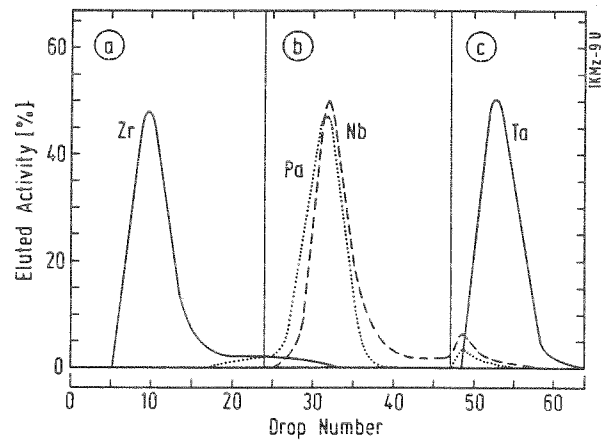

Figure 2: Separation of Zr, Nb and Pa, and Ta on a 1.7 x 11mm TIOA/VOLTALEF column. Eluens : a) 12 M HCl/0.02 M HF , b) 4 M HCl/0.02 M HF c) 6 M HNO_3/0.015 M HF.

ARCA II - A New Apparatus for Fast, Repetitive Element 105 Separations [G]

M. Schädel, W. Brüchle, E. Jäger, E. Schimpf
GSI Darmstadt
J.V. Kratz, P. Zimmermann, U.W. Scherer
Institut für Kernchemie, Universität Mainz

In proceeding with our studies of the chemical properties of the heaviest actinide element Lawrencium to the transactinide elements we have to cope with the decreasing half-lives of the longest lived isotopes dropping down from 3 minutes for the isotope ^{260}Lr to 35 s for ^{262}105. While we had successfully used our Automated Rapid Chemistry Apparatus (ARCA)[1] for fast radiochemical separations of isotopes in the minute half-life range, this apparatus still had the disadvantages of having not only rather large dead-volumes because of all the tubing connections between the valves and columns which were mounted separately, but also a standard fitting technique to mount the column was used which prevented us from a fast, repetitive change of columns from one separation to the next. To overcome this drawback and to study isotopes with half-lives of only some tens of seconds, like the 35s ^{262}105, we have built a newly designed version of our ARCA system. In the following, this apparatus, ARCA II, will briefly be described while preliminary results from our investigation of the isotope ^{262}105 is given elsewhere in this report [2,3].

All processes in ARCA II were electronically controlled by a GSI 85-microcomputer and electro-pneumatic valves as they have been used before[1]. We again have used BASIC as a programming language and time-command sequences in the program to control the separations.

The following two major changes from our previous apparatus have been made : firstly, we integrated all components of the apparatus which contribute to dead volumes, and consequently to longer separation times, into one very compact unit, and therein we kept these dead volumes to a minimum by using short and very narrow bore holes with a diameter of 0.3 mm to connect the individual parts, and secondly, we imbedded two times 20 micro separation columns, as small as 1.6 × 8 mm each, into two remotely controlled movable magazines. As a result we were able to reduce the dead volume, including that of the column, to about 35 μl, and we could change columns within a fraction of a second. Therefore, we not only had to build the individual parts with a high precision to fit the narrow bores together but the positioning of all movable parts had to be performed with a precision of 0.1 mm or better. All seals inside the separation unit were made by pressing polished surfaces of Kel-F against Teflon or by using O-rings. Chemically inert materials had to be used throughout because highly corrosive mineral acids (HCl, HF, HNO_3) were required as solvents.

The middle sectional plane of our ARCA II apparatus is shown in figure 1. Reaction products attached to KCl aerosols, JET, were collected on a polyethylene frit, F, with a 35 μm pore diameter while the carrier gas was pumped through into an exhaust line. To dissolve the activity from the frit and to load it onto the separation column, C, in the first solvent stream, I, a slider, SF, was pushed to the left, and a new collection period of products began on the second frit.

Slider valves [1] which were mounted in a close geometry on top of the unit shown in figure 1, were used for a fast change of solvents in the course of the separation. Downstream the separation columns sliders, S, were used to direct undesired solvent volumes through tubings to the rear side into the waste, W, or to collect fractions of interest on Ta-discs. Samples were prepared by a fast evaporation procedure with a spot infra-red heat lamp. After the separation has been finished on the left column, the top slider, SF, was moved to the right to immediately start a new separation on the right column. Simultaneously, the left magazine, M, which carries 20 columns, was pushed forward to bring a new column into position.

About 1600 experiments with a cycle time of 1 min each were performed to separate individual fractions of Nb, Pa, and Ta, and to separate these, including element 105, from undesired interferring actinides by use of this micro-HPLC.

1. M. Schädel et al., Nucl. Instr. and Meth. A264, 308 (1988).
2. J.V. Kratz et al., contribution to this report.
3. U.W. Scherer et al., contribution to this report.

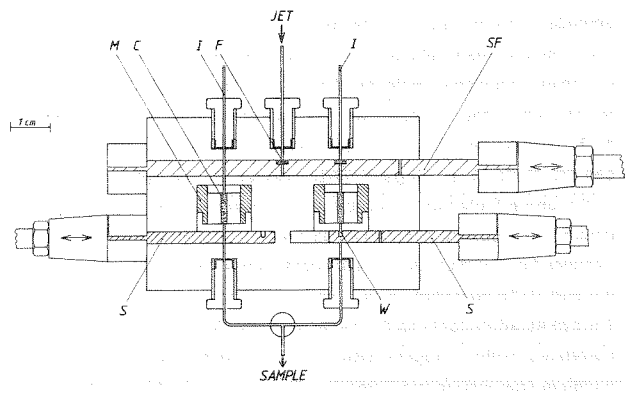

Fig.1:

View of the middle sectional plane of ARCA II (M - magazine with columns, C - separation column, I - inlet tube for solvents, F - frit in position to collect reaction products, SF - slider with frits, S - slider, on the left hand side in position for sample collections, W - tubing connection through the rear side into the waste).

Chemical Properties of Element 105 in Aqueous Solution: Halide Complex Formation and Anion Exchange into Tri-Isooctyl Amine [B]

J.V. Kratz, S. Zauner, H.P. Zimmermann, U.W. Scherer
Institut für Kernchemie, Universität Mainz
M. Schädel, W. Brüchle, B. Schausten
GSI Darmstadt
C.M. Gannett, K.E.Gregorich, H.L. Hall, R.A. Henderson,
D.M. Lee, M.J. Nurmia, D.C. Hoffman
Lawrence Berkeley Laboratory, Berkeley
U. Baltensperger, H. Gäggeler, D. Jost, Ya Nai-Qi
PSI, Würenlingen
Ch. Lienert, A. Türler
Universität Bern

The chemical properties of element 105, hahnium, in aqueous solution are expected to be analogous to those for the group-5 elements, and trends in chemical properties between niobium and tantalum are expected to continue, allowing extrapolation to the chemical properties of hahnium as the heaviest group-5 element. Recently, the LBL group conducted experiments [1] which showed indeed that hahnium has chemical properties similar to those of niobium and tantalum: It adhered to glass surfaces upon fuming with nitric acid, a property very characteristic of the group-5 elements. However, some unexpected differences between tantalum and hahnium were found in their fluoride-complexing behaviour and subsequent extraction into methyl isobutyl ketone.

In order to further explore the unusual halide-complexing behaviour of hahnium, we performed liquid-liquid extraction studies [2] in the hydrochloric acid/Tri-isooctyl amine (TIOA) system using our miniaturized computer-controlled chromatographic column apparatus ARCA II [3].

The longest lived isotope of element 105, 35-s ^{262}Ha, was produced at the LBL 88-inch cyclotron in the $^{249}Bk(^{18}O,5n)$ reaction, and transported on-line by a He/KCl-jet to the chemistry apparatus where it was collected on a polyethylene frit. After a collection time of 60 s the frit was washed with 10 M or 12 M HCl which dissolved the activities, and assured chloride complexing of the group-5 elements. This solution passed through one of the TIOA/Voltalef mini columns (1.6 × 8 mm) where the homologs Nb and Ta, as well as the pseudo-member of group 5, Pa, were extracted [2], while the group-4 elements and the actinides were eluted from the column.

In a first series of about 200 experiments designed to verify that the extraction of halide complexes of hahnium into TIOA was accomplished at all, after the feeding of the activities onto the column in 12 M HCl/0.02 M HF and the subsequent elution of the actinides (An), see top of Fig. 1, the organic phase containing the halide complexes of the group-5 elements was dissolved in acetone, stripped from the column, and quickly evaporated to dryness on Ta disks. Assay of the samples for α-particle decay and spontaneous fission started 45 s after the end of the collection cycle. The observation in the acetone strip of 9 α events attributable to the decay of $^{262}Ha/^{258}Lr$, among these 1 time-correlated mother-daughter pair, and of 12 fission events, assured that hahnium was indeed extracted into the amine with high yield. Similarly, it was found that hahnium is also extracted from 10 M HCl in the absence of hydrofluoric acid. The elution curves in Fig. 1 were obtained by using isotopes of Pm (a homolog of the actinides (An)), Zr, and Hf (both eluting from the column in an identical manner as Pm, not shown in Fig. 1), and Nb and Ta freshly produced on-line and subjected to the same chemical procedures used for the hahnium separations.

Next, in a series of 721 collection and separation cycles, after feeding of the activities onto the column, we performed separate elutions of a Nb/Pa fraction and a Ta fraction, as shown in the middle of Fig. 1. 42 α-events due to $^{262}Ha/^{258}Lr$ were registered in the Nb/Pa fraction, and only 5 α-decays in the Ta fraction! This distribution is identical with the behaviour of Nb and Pa, but not with that of Ta. Apparently, in contrast to simple extrapolations, the trend in the chemical properties of the group-5 elements from Nb to Ta does not continue but is reversed in going from Ta to Ha.

Finally, in a series of 536 experiments, a separation of Pa from Nb was performed (bottom of Fig. 1) with the hahnium decays (52 α events, including 10 correlated pairs, and 45 fission events) being evenly distributed between both fractions, thus indicating that the halide complexing in 10 M HCl/0.025 M HF and the subsequent amine extraction is stronger with Ha than with Pa but weaker than with Nb.

It remains to be seen whether calculations of the chemical properties of element 105 are capable of reproducing these observations.

1. K.E. Gregorich et al., Radiochimica Acta, **43**, 223 (1988)
2. H.P. Zimmermann et al., contribution to this report
3. M. Schädel et al., contribution to this report

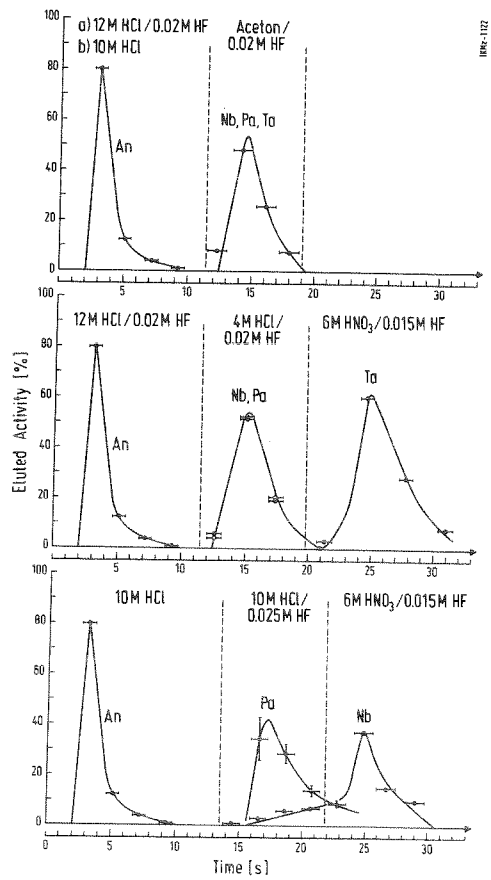

Fig. 1: Elution of the actinides (An), of Nb, Pa, and Ta from a tri-isooctyl amine column as a function of time in three series of experiments. The distribution of the ^{262}Ha activity among the various fractions is detailed in the text.